analyses with DNA microarrays to identify genes that are downstream of *twist* in mesoderm development. These efforts should be helpful in gaining a comprehensive view of cell fate determination, organogenesis, cell proliferation, and pattern formation in the mesoderm.

References and Notes

1. B. Thisse, M. el Messal, F. Perrin-Schmitt, *Nucleic Acids Res.* **15**, 3439 (1987).
2. M. Leptin, B. Grunewald, *Development* **110**, 73 (1990).
3. O. M. Borkowski, N. H. Brown, M. Bate, *Development* **121**, 4183 (1995).
4. M. K. Baylies, M. Bate, *Science* **272**, 1481 (1996).
5. J. Spring *et al.*, *Dev. Biol.* **228**, 363 (2000).
6. M. V. Taylor, K. E. Beatty, H. K. Hunter, M. K. Baylies, *Mech. Dev.* **50**, 29 (1995).
7. Z. Yin, X. L. Xu, M. Frasch, *Development* **124**, 4971 (1997).
8. N. D. Hopwood, A. Pluck, J. B. Gurdon, *Cell* **59**, 893 (1989).
9. C. Wolf *et al.*, *Dev. Biol.* **143**, 363 (1991).
10. S. M. Wang *et al.*, *Gene* **187**, 83 (1997).
11. M. V. Taylor, *Curr. Biol.* **10**, R646 (2000).
12. M. Bate, Ed., in *The Development of* Drosophila melanogaster (Cold Spring Harbor Laboratory Press, Plainview, NY, 1993), vol. II, pp. 1013–1090.
13. Web figures 1 through 3, Web table 1, and supplemental text are available at *Science* Online at www.sciencemag.org/cgi/content/full/1062660/DC1.
14. D. Casso, F. Ramirez-Weber, T. B. Kornberg, *Mech. Dev.* **91**, 451 (2000).
15. E. E. Furlong, D. Profitt, M. P. Scott, *Nature Biotechnol.* **19**, 153 (2001).
16. J. A. Campos-Ortega, V. Hartenstein, *The Embryonic Development of* Drosophila melanogaster (Springer-Verlag, Germany, 1997), pp. 9–84.
17. V. G. Tusher, R. Tibshirani, G. Chu, *Proc. Natl. Acad. Sci. U.S.A.* **98**, 5116 (2001).
18. P. Tamayo *et al.*, *Proc. Natl. Acad. Sci. U.S.A.* **96**, 2907 (1999).
19. S. Vincent, R. Wilson, C. Coelho, M. Affolter, M. Leptin, *Mol. Cell* **2**, 515 (1998).
20. S. K. Doberstein, R. D. Fetter, A. Y. Mehta, C. S. Goodman, *J. Cell. Biol.* **136**, 1249 (1997).
21. P. Armand, A. C. Knapp, A. J. Hirsch, E. F. Wieschaus, M. D. Cole, *Mol. Cell. Biol.* **14**, 4145 (1994).
22. A. Lakey *et al.*, *EMBO J.* **12**, 2863 (1993).
23. D. S. Schneider, K. L. Hudson, T. Y. Lin, K. V. Anderson, *Genes Dev.* **5**, 797 (1991).
24. M. P. Belvin, K. V. Anderson, *Annu. Rev. Cell. Dev. Biol.* **12**, 393 (1996).
25. I. Gross, P. Georgel, C. Kappler, J. M. Reichhart, J. A. Hoffmann, *Nucleic Acids Res.* **24**, 1238 (1996).
26. J. Casal, M. Leptin, *Proc. Natl. Acad. Sci. U.S.A.* **93**, 10327 (1996).
27. M. B. Eisen, P. T. Spellman, P. O. Brown, D. Botstein, *Proc. Natl. Acad. Sci. U.S.A.* **95**, 14863 (1998).
28. M. Leptin, *Genes Dev.* **5**, 1568 (1991).
29. M. Levine, *Cell* **52**, 785 (1988).
30. M. Frasch, *Nature* **374**, 464 (1995).
31. K. Staehling-Hampton, F. M. Hoffman, M. K. Baylies, E. Rushton, M. Bate, *Nature* **372**, 783 (1994).
32. R. Reuter, B. Grunewald, M. Leptin, *Development* **119**, 1135 (1993).
33. P. T. Chuang, T. B. Kornberg, *Curr. Opin. Genet. Dev.* **10**, 515 (2000).
34. J. R. Kennerdell, R. W. Carthew, *Cell* **95**, 1017 (1998).
35. G. M. Cann, J. W. Lee, F. E. Stockdale, *Anat. Embryol.* **200**, 239 (1999).
36. K. E. Lewis, *et al.*, *Dev. Biol.* **216**, 469 (1999).

37. We thank E. Johnson, M. Arbeitman, B. Baker, M. Siegal, R. Tibshirani, and V. Goss Tusher for statistical advice; B. Baker, F. Imam, and G. Zimmermann for careful manuscript reading; and M. Arbeitman, F. Imam, and E. Johnson for collaborating to prepare the arrays and reference sample. Support for E.F. by European Molecular Biology Organization and Stanford Berry Fellowships, B.N. by NSF, and K.W. by Helen Hay Whitney fellowships. The research was supported by NIH grant K22 HG00045-02 (K.W.) and HHMI and Defense Advanced Research Projects Agency grant MDA-972-00-1-0032 (M.S.).

18 May 2001; accepted 23 July 2001
Published online 2 August 2001;
10.1126/science.1062660
Include this information when citing this paper.

Origin of the Hard X-ray Emission from the Galactic Plane

Ken Ebisawa,[1*] Yoshitomo Maeda,[2,3] Hidehiro Kaneda,[3] Shigeo Yamauchi[4]

The Galactic plane is a strong emitter of hard x-rays (2 to 10 kiloelectron volts), and the emission forms a narrow continuous ridge. The currently known hard x-ray sources are far too few to explain the ridge x-ray emission, and the fundamental question of whether the ridge emission is ultimately resolved into numerous dimmer discrete sources or truly diffuse emission has not yet been settled. In order to obtain a decisive answer, using the Chandra X-ray Observatory, we carried out the deepest hard x-ray survey of a Galactic plane region that is devoid of known x-ray point sources. We detected at least 36 new hard x-ray point sources in addition to strong diffuse emission within a 17′ by 17′ field of view. The surface density of the point sources is comparable to that at high Galactic latitudes after the effects of Galactic absorption are considered. Therefore, most of these point sources are probably extragalactic, presumably active galaxies seen through the Galactic disk. The Galactic ridge hard x-ray emission is diffuse, which indicates omnipresence within the Galactic plane of a hot plasma, the energy density of which is more than one order of magnitude higher than any other substance in the interstellar space.

The Galactic ridge x-ray emission exhibits emission lines from highly ionized heavy elements such as Si, S, and Fe; hence, it may be considered to originate from optically thin hot plasmas with a temperature of several keV (*1*). If the plasma distribution is diffuse in the Galactic disk, the plasma temperature is higher than that which can be bound by Galactic gravity (*2*), and its energy density, $\sim$10 eV/cm^3, is one or two orders of magnitude higher than those of other constituents in the interstellar space, such as cosmic rays, Galactic magnetic fields, and ordinary interstellar medium (*1, 3*). Another hypothesis is that the Galactic ridge x-ray emission is a superposition of numerous point sources (*4–7*). However, no class of x-ray objects is known with such a high plasma temperature and a large number density to satisfy the uniform surface brightness of the ridge emission (*3, 8*).

To resolve the origin of the Galactic ridge x-ray emission, we observed a "blank" region of the Galactic plane, $(l,b) \approx (+28°.45, -0°.2)$, where the Advanced Satellite for Cosmology and Astrophysics (ASCA) could not find any point sources (*3, 9*) brighter than $\sim 2 \times 10^{-13}$ erg s^{-1} cm^{-2} (2 to 10 keV). We used the Advanced CCD Imaging Spectrometer Imaging (ACIS-I) array on board the Chandra X-ray Observatory, with unprecedented sensitivity and imaging quality (Fig. 1). The observation was carried out on 25 and 26 February 2000, for a total exposure time of 90 ks. The pointing position was chosen because the direction is tangential to the Scutum arm where the ridge x-ray emission is strong.

We were interested in hard x-ray emission, so we searched in the 3- to 8-keV band to minimize the effects of Galactic absorption at lower energies and the intrinsic non–x-ray background in the higher energy band. The "wavdetect" source finding program in the Chandra data analysis package detected 53, 36, and 29 sources in the 17′ by 17′ ACIS-I field with 3σ, 4σ, and 4.5σ significance, respectively. For each of these sources, we determined the energy flux in the 2- to 10-keV band by fitting the energy spectrum after accounting for the position-dependent detector responses. The 3σ, 4σ, and 4.5σ thresholds roughly correspond to energy fluxes of $\sim 3 \times 10^{-15}$, $\sim 4 \times 10^{-15}$, and $\sim 5 \times 10^{-15}$ ergs s^{-1} cm^{-2} in the 2- to 10-keV band, respectively. We found that point sources with different fluxes are randomly distributed over the field of view, which indicates that the positional dependence of the source detection efficiency is negligible. We also carried out a source search in the 0.5- to 3-keV soft x-ray band and detected 106 sources with 3σ confidence. There are only 17 sources that are detected both in the hard and soft band over 3σ confidence, which suggests that the populations of the soft and hard sources are different. We identified several soft x-ray sources, which are not detected in the hard band, with objects in the United States Naval Observatory A2.0 catalog and/or the Palomar Digital Deep Sky Survey; thus, these sources are probably ordinary stars. On the other hand, none of the hard x-ray sources we observed have been identified.

Chandra data consist of not only x-ray events from point sources and diffuse emission, but also non–x-ray background events. The typical non–x-ray background rate has been calculated and released by the Chandra X-ray Observatory Center, and is based on observations of source-free high Galactic latitude regions. By subtracting the expected non–x-ray background rate, we determined the total hard x-ray flux in our field of view as $\sim 1.1 \times 10^{-10}$ ergs s^{-1} cm^{-2} deg^{-2} in the 2- to 10-keV band, which includes contributions from both diffuse emission and point sources. However, integrated hard x-ray flux of all the point sources above the flux 3×10^{-15} ergs s^{-1} cm^{-2} is $\sim 9.8 \times 10^{-12}$ ergs s^{-1} cm^{-2} deg^{-2} (2 to 10 keV), which is only ~10% of the total observed x-ray flux in the field of view, and the rest is the diffuse emission (Figs. 1 and 2).

The point x-ray sources on the Galactic plane may comprise extragalactic sources seen through the Galactic plane and Galactic sources. Remarkably, the surface density of the hard x-ray sources on the Galactic plane we have determined is consistent with that of the high Galactic latitude fields in a similar flux range (Fig. 2). The x-ray fluxes of extragalactic sources are reduced on the Galactic plane, because they are absorbed by interstellar matter. The Galactic HI column density in our Chandra pointing direction is $\sim 2 \times 10^{22}$ cm^{-2} (*10*) and that of molecular hydrogen is 1×10^{22} to 2×10^{22} cm^{-2} (*11*), both measured from radio observations (*10, 11*). Therefore, the total hydrogen column density through the Galactic plane is $N_H = N_{HI} + 2N_{H2} = 4 \times 10^{22}$ to 6×10^{22} cm^{-2}. Even if we account for the ~30% flux reduction of the extragalactic hard x-ray sources caused by the interstellar absorption of $N_H = 6 \times 10^{22}$ cm^{-2}, the extragalactic log$N$ − log$S$ curve is still consistent with the present Chandra Galactic log$N$ − log$S$ curve within 90% statistical uncertainty (Fig. 2). Therefore, most of the point sources detected in our field must be extragalactic, presumably active galactic nuclei, which dominate the cosmic x-ray background (*12*).

From our observation, the point source density on the Galactic plane in the flux range above 3×10^{-15} ergs s^{-1} cm^{-2} (2 to 10 keV) is 660 ± 160 sources/degree^2 (90% error), among which ~560 sources/degree^2 are considered to be the extragalactic sources (*12*), where we took account of the ~30% flux reduction due to the Galactic absorption. This suggests that there would be at most ~260 sources/degree^2 Galactic sources at this flux level, which corresponds to a $\sim 4 \times 10^{31}$ erg s^{-1} source at 10 kiloparsec (kpc) assuming isotropic emission. X-ray luminosity functions and spatial densities of quiescent dwarf novae have not been measured precisely (*5, 7*), and our results can place an upper limit for the

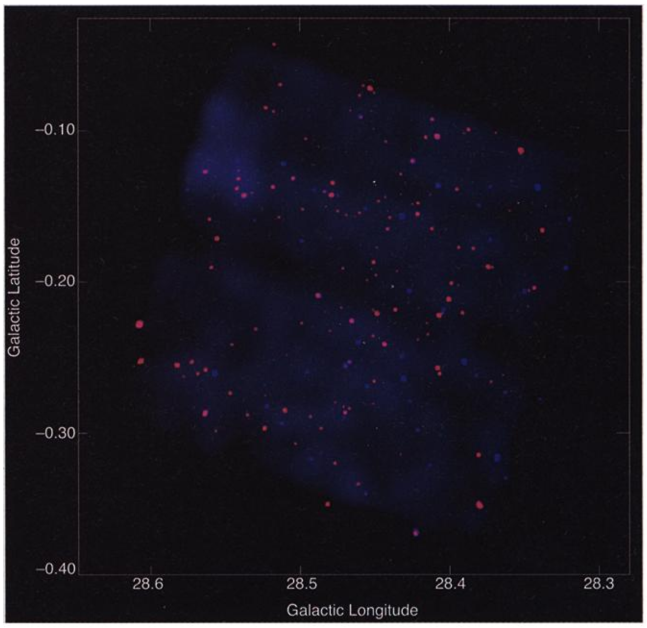

Fig. 1. The Chandra ACIS-I deep exposure image on the Galactic plane. The original image has been smoothed with an adaptive filter to make both the point sources and diffuse emission clearly visible. Color and contrast are adjusted so that the point sources detected in the 0.5- to 3-keV band and the 3- to 8-keV band are conspicuous in red and blue, respectively. The hard x-ray diffuse emission is shown in blue. The image is 900 pixels by 900 pixels with the pixel size 1.″48 square.

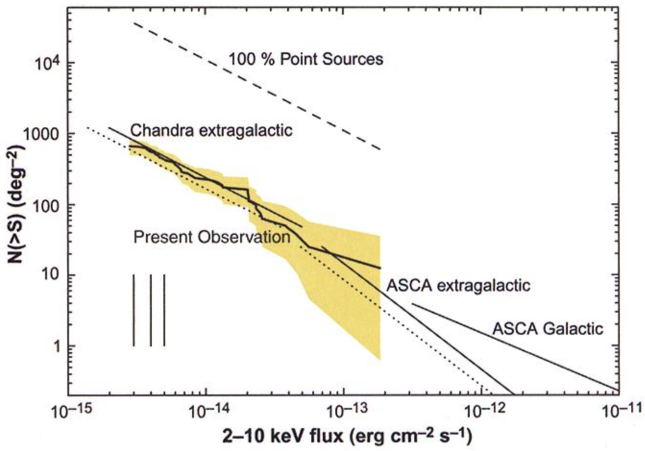

Fig. 2. The number of point sources per unit area, N, brighter than the threshold flux in the 2- to 10-keV band, S, is indicated as a function of S (the log$N$ − log$S$ curve). The present Chandra log$N$ − log$S$ curve on the Galactic plane is shown with the thick solid line, and the 90% error region (assuming Poisson counting error) is indicated in yellow. The upper dashed line shows the number of fictitious point sources at a given flux S that would have accounted for the total observed x-ray energy flux in the Chandra field of view ($\sim 1.1 \times 10^{-10}$ ergs s^{-1} cm^{-2} deg^{-2} in the 2- to 10-keV band). Three vertical lines at lower left indicate the threshold energy fluxes corresponding to 3σ, 4σ, and 4.5σ confidence of the source detection. For comparison, the Galactic log$N$ − log$S$ curve by ASCA (*8*), and extragalactic ones by Chandra (*12*) and ASCA (*21*) are shown. The extragalactic log$N$ − log$S$ curves corrected for the effect of ~30% flux reduction due to Galactic absorption with $N_H = 6 \times 10^{22}$ cm^{-2} are indicated with dotted lines, which are consistent with the present Galactic log$N$ − log$S$ curve within 90% statistical error.

[1]Code 662, NASA Goddard Space Flight Center, Greenbelt, MD 20771, USA, and Universities Space Research Association, Seabrook, MD 20706, USA. [2]Department of Astronomy and Astrophysics, Pennsylvania State University, 525 Davey Laboratory, University Park, PA 16802, USA. [3]Institute of Space and Astronautical Science, 3-1-1 Yoshinodai, Sagamihara, Kanagawa 229-8510, Japan. [4]Faculty of Humanities and Social Sciences, Iwate University, 3-18-34 Ueda, Morioka, Iwate 020-8550, Japan.

*To whom correspondence should be addressed. E-mail: ebisawa@gsfc.nasa.gov

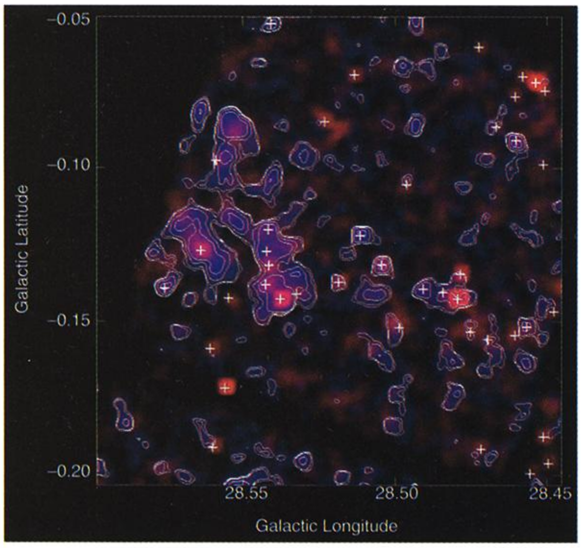

Fig. 3. Close-up of the diffuse feature at around $(l,b) \approx (28°.55, -0°.12)$. The 0.5- to 3-keV image is represented in red, the 3- to 8-keV image is in blue, and both images are smoothed to enhance the diffuse feature. A contour map of the 3- to 8-keV image is superimposed. Point sources detected with more than 3σ confidence either in the 0.5- to 3-keV band or the 3- to 8-keV band are indicated with crosses. The image is 560 pixels by 560 pixels with the pixel size 0.″98 square.

quiescent dwarf nova population. For example, a combination of a 10^{-5} pc^{-3} spatial density and 10^{31} erg s^{-1} average luminosity of quiescent dwarf novae, which amounts to ~1000 sources/degree^2 at $>3 \times 10^{-15}$ ergs s^{-1} cm^{-2} (*9*), is clearly ruled out. To be consistent with our observation, either spatial density or average luminosity has to be smaller at least by a factor of 4.

The paucity of Galactic point sources supports models of diffuse emission to explain the Galactic ridge x-ray emission. Then, the next question is how to produce plasmas with such a large energy density and high temperatures, and keep them in the Galactic disk. Theories have been proposed to explain these problems in terms of interstellar-magnetic reconnection (*13*), or interaction of energetic cosmic-ray electrons (*14*) or heavy ions (*15*) with interstellar medium. All of these models require supernovae as a mechanism of the energy input. Incidentally, in the region around $(l,b) \approx (28°.55, -0°.12)$, we found an extended feature with a size of ~2′, which is more conspicuous in the hard x-ray band than in the soft band (Fig. 3). This region corresponds to the southern end of an extended and patchy radio source named G28.60-0.13 (*16*), and the diffuse x-ray structure we found bridges three discrete radio patches: F, G, and H (*16*). A high-quality x-ray spectrum of the G28.60-0.13 region by the ASCA satellite indicates that the energy spectrum is a single power law without any iron line emissions (*17*), reminiscent of the nonthermal acceleration taking place in the supernova remnants suchas SN1006 (*18*) or RX J1713.7-3946 (*19*).The extended feature at $(l,b) \approx (28°.55, -0°.12)$, or G28.60-0.13 itself, may be an aged supernova remnant. Supernova remnants may be ubiquitous on the Galactic plane (*16*), and these remnants may have an important role in generating the Galactic ridge hard x-ray emission (*20*).

References and Notes

1. K. Koyama *et al.*, *Publ. Astron. Soc. Jpn.* **38**, 121 (1986).
2. R. S. Warwick, M. J. L. Turner, M. G. Watson, R. Wilingale, *Nature* **317**, 218 (1985).
3. H. Kaneda *et al.*, *Astrophys. J.* **491**, 638 (1997).
4. D. M. Worrall, F. E. Marshall, E. A. Boldt, J. H. Swank, *Astrophys. J.* **255**, 111 (1982).
5. K. Mukai, K. Shiokawa, *Astrophys. J.* **418**, 863 (1993).
6. R. Ottmann, J. H. M. M. Schmitt, *Astron. Astrophys.* **256**, 421 (1992).
7. M. G. Watson, in *Annapolis Workshop on Magnetic Cataclysmic Variable*, ASP Conference Series, vol. 157, C. Hellier, K. Mukai, Eds. (Astronomical Society of the Pacific, San Francisco, 1999), p. 291.
8. M. Sugizaki *et al.*, *Astrophys. J. Suppl.* **134**, 77 (2001).
9. S. Yamauchi *et al.*, *Publ. Astron. Soc. Jpn.* **48**, L15 (1996).
10. J. M. Dickey, F. J. Lockman, *Annu. Rev. Astron. Astrophys.* **28**, 215 (1990).
11. T. M. Dame, D. Hartmann, P. Thaddeus, *Astrophys. J.* **547**, 792 (2001).
12. R. Giacconi *et al.*, *Astrophys. J.* **551**, 624 (2001).
13. S. Tanuma *et al.*, *Publ. Astron. Soc. Jpn.* **51**, 161 (1999).
14. A. Valinia *et al.*, *Astrophys. J.* **543**, 733 (2000).
15. Y. Tanaka, T. Miyaji, G. Hasinger, *Astron. Nachr.* **320**, 181 (1999).
16. D. J. Helfand, T. Velusamy, R. H. Becker, F. J. Lockman, *Astrophys. J.* **341**, 151 (1989).
17. A. Bamba *et al.*, *Publ. Astron. Soc. Jpn.* **53**, accepted (2001).
18. K. Koyama *et al.*, *Nature* **378**, 255 (1995).
19. K. Koyama *et al.*, *Publ. Astron. Soc. Jpn.* **49**, L7 (1997).
20. K. Koyama, S. Ikeuchi, K. Tomisaka, *Publ. Astron. Soc. Jpn.* **38**, 503 (1986).
21. Y. Ueda *et al.*, *Astrophys. J.* **518**, 656 (1999).

22. We are grateful to F. E. Marshall, K. Mukai, and R. F. Mushotzky for helpful comments that improved an earlier version of this report. We also thank Y. Tanaka and other anonymous referees for useful comments. The observation was carried out under NASA's Chandra Guest Observer Program.

18 June 2001; accepted 30 July 2001
Published online 9 August 2001;
10.1126/science.1063529
Include this information when citing this paper.

Spatiotemporal Self-Organization in a Surface Reaction: From the Atomic to the Mesoscopic Scale

C. Sachs, M. Hildebrand, S. Völkening, J. Wintterlin,* G. Ertl

Scanning tunneling microscopy data revealed the atomic processes in propagating reaction fronts that occur in the catalytic oxidation of hydrogen on Pt(111). The fronts were also characterized on mesoscopic length scales with respect to their velocity and width. Simulations on the basis of a reaction-diffusion model reproduce the experimental findings qualitatively well. The quantitative comparison reveals the limitations of this traditional approach to modeling spatiotemporal pattern formation in nonlinear dynamics.

Spatiotemporal pattern formation in open systems far from equilibrium is the basis of self-organization of matter. Catalytic reactions between small molecules on well-defined solid surfaces are probably the simplest model systems that show such phenomena (*1*). Concentration patterns are formed on mesoscopic length scales (typically 1 μm to 1 mm) that can be imaged with techniques such as photoemission electron microscopy (*2*). Nonequilibrium patterns can be observed if the reaction kinetics fulfill certain criteria. The minimum requirements are the presence of nonlinearities and of spatial coupling. These patterns can be modeled with reaction-diffusion (RD) equations (*3, 4*), in which the properties of the individual particles are replaced by continuum variables such as adsorbate concentrations, and this approach often provides a good qualitative description. Fluctuations are usually neglected because the atomic scale (<1 nm) is much smaller than the typical length scale of the observed patterns.

Fritz-Haber-Institut der Max-Planck-Gesellschaft, D-14195 Berlin, Germany.

*To whom correspondence should be addressed. E-mail: wintterlin@fhi-berlin.mpg.de